Distribution-free stochastic model updating of dynamic systems with parameter dependencies

Masaru Kitahara [a, *], **Sifeng Bi** [b], **Matteo Broggi** [a], **Michael Beer** [a, c, d]

[a] *Leibniz Universität Hannover, Institute for Risk and Reliability, Hannover, Germany*

[b] *University of Strathclyde, Department of Mechanical & Aerospace Engineering, Aerospace Centre of Excellence, Glasgow, United Kingdom*

[c] *University of Liverpool, Institute for Risk and Uncertainty, Liverpool, United Kingdom*

[d] *Tongji University, International Joint Research Center for Engineering Reliability and Stochastic Mechanics, Shanghai, China*

* Correspondence author. E-mail address: masaru.kitahara@irz.uni-hannover.de (M. Kitahara).

Abstract: This work proposes a distribution-free stochastic model updating framework to calibrate the joint probabilistic distribution of the multivariate correlated parameters. In this framework, the marginal distributions are defined as the staircase density functions and the correlation structure is described by the Gaussian copula function. The first four moments of the staircase density functions and the correlation coefficients are updated by an approximate Bayesian computation, in which the Bhattacharyya distance-based metric is proposed to define an approximate likelihood that is capable of quantifying the discrepancy between model outputs and measurement data. The feasibility of the framework is demonstrated on two illustrative examples and a followed real-world application to a nonlinear dynamic system updating problem based on measured time signals. The results indicate the importance of considering the parameter dependencies in stochastic model updating.

1. Introduction

The model updating has been developed as a fascinating technique to mitigate the discrepancy between model outputs and experimental measurements [1,2]. The causes of the discrepancy during the model updating can be generally classified into following three categories:

- Parameter uncertainty. Model parameters, e.g., geometry dimensions, boundary conditions, and material properties, often cannot be exactly determined;
- Modelling uncertainty. Simplifications or approximations, e.g., linearization and frictionless mechanical joints, have to be made to numerically represent the physical system;
- Measurement uncertainty. Measured quantities are inevitably contaminated by the hard-to-control randomnesses, e.g., environmental noises and measurement system errors.

The deterministic model updating, especially for the sensitivity method [1], might be one of the most successful model updating techniques. It aims at calibrating the model parameters to find their optimal values from a single set of measurements. It has been employed in a wide range of practical applications, including the correction of large-scale finite element (FE) models [3,4]. Nevertheless, it accounts for measurement data as an exactly determined values/signals, with no consideration of the measurement uncertainty.

Comparatively, the stochastic model updating, including the perturbation method [5,6], Monte Carlo method [7,8], and Bayesian method [2,9], can be interpreted as the techniques to calibrate not the parameters themselves but the uncertainty characteristics, i.e., probabilistic distributions, so that the model outputs are committed not to the maximum fidelity to a single set of measurements but to the uncertainty characteristics of the multiple sets of measurements. In the stochastic model updating,

46 uncertainty quantification (UQ) metrics play a key role to quantify the statistical discrepancy between
47 the model outputs and measurements because of the above three sources of uncertainty. A series of
48 distances, such as the Euclidian distance, Mahalanobis distance, and Bhattacharyya distance has been
49 successfully proposed to define the UQ metrics in the stochastic model updating [8]. In addition, the
50 Frobenius norm has been also utilized to define the UQ metric to quantify the difference between the
51 covariance matrices of the model outputs and measurements [10]. Bi et al. [11] has recently developed
52 a Bayesian updating framework employing the approximate Bayesian computation (ABC) technique
53 [12,13], where the Bhattacharyya distance-based approximate likelihood is used. This framework has
54 been demonstrated to be capable to calibrate numerical models such that the model outputs recreate
55 wholly the uncertainty characteristics of target measurements. The framework has been furthermore
56 extended to the calibration of dynamic systems, so that the procedure enables to quantify wholly the
57 uncertainty characteristics of the measured time signals [14].
58   In the stochastic model updating, distribution families of the parameters commonly need to be
59 assigned a priori, then the prior distribution of the hyper-parameters such as means and variances is
60 updated to the posterior distribution using the measurement data. The distribution families, however,
61 are often unknown beforehand due to the scarce and/or incomplete available data for the parameters.
62 The newly released NASA UQ challenge problem 2019 [15], for instance, requires a model calibration
63 task in an extremely challenging condition that no distribution information of the aleatory parameters
64 is provided other than a common bounded support domain. In such situation, the assumption on the
65 distribution formats might significantly affect the model updating results. Therefore, Kitahara et al.
66 [16] has recently developed a distribution-free Bayesian updating framework, where staircase density
67 functions [17] are assigned to the underlying distribution families of the parameters. Staircase density
68 functions enable to flexibly approximate a broad range of distributions arbitrary close, such as highly
69 skewed and/or multi-modal distributions, and are hence particularly appropriate to characterize the
70 parameters whose density formats cannot be specified. The framework has been demonstrated to be
71 capable to calibrate the probabilistic distribution of the parameters without limiting hypotheses upon
72 the distribution families.
73   Nevertheless, the aforementioned distribution-free updating framework still has open questions.
74 Firstly, the framework has been currently only demonstrated on the updating by scalar-valued modal
75 responses. Hence, in this study, it is extended to the updating of dynamic systems by measured time
76 signals. Secondly, staircase density functions are provided for univariate random variables, and thus
77 cannot consider the parameter dependencies, which might lead to inaccurate updating results in the
78 presence of strong correlation among parameters. Copula functions are well-known to be capable to
79 provide an effective way to characterize the dependence structure among parameters, and have been
80 widely applied to reliability problems [18-20]. Among various types of copula functions, the Gaussian
81 copula function is most widely used because it can be easily generalized to the multivariate case, and
82 this property is particularly attractive for the stochastic model updating problem, in which very large
83 number of parameters is considered as random variables.
84   The objective of this work is consequently to develop a stochastic model updating framework to
85 calibrate the joint probability distribution of the correlated parameters without prior knowledge on
86 the distribution families of the marginal distributions. In order to achieve this task, it is assumed that
87 the joint probability distribution of the parameters is characterized by a combination of the Gaussian
88 copula function and staircase density functions. Moment constraints for the existence of the staircase
89 density functions and the correlation coefficient constraint for the existence of the copula function are
90 then derived. Furthermore, the Bhattacharyya distance is utilized to define an approximate likelihood
91 function quantifying the stochastic discrepancy between the model outputs and measurements, such
92 that the hyper-parameters of the staircase density functions as well as the correlation coefficients of
93 the copula function are calibrated through an ABC updating approach. The proposed framework is
94 first demonstrated on both bi-variate and multi-variate cases using two simple illustrative examples,
95 and then applied to a model updating problem of a seismic-isolated bridge pier model based on the
96 simulated seismic response data, so as to demonstrate the feasibility of the framework in the updating
97 of nonlinear dynamic systems.

98   The structure of this paper is as follows. Section 2 first describes theoretical and methodological
99   bases of the three key ingredients of the proposed framework, i.e., the Bhattacharyya distance-based
100 UQ metrics, staircase density functions, and Gaussian copula function. Then, in Section 3, we outline
101 the formulation of the Bayesian updating with the combination of the Gaussian copula function and
102 staircase density functions, and the proposed ABC updating framework. Illustrative applications are
103 provided in Section 4, employing a simple shear building model and a spring-mass system, and the
104 feasibility of the proposed framework in the updating of nonlinear dynamic systems by the measured
105 time signals is further demonstrated in Section 5. Finally, Section 6 gives conclusions to this paper.

2. Theories and methodologies

2.1. Bhattacharyya distance-based UQ metrics

108   The system under investigation in the stochastic model updating is described as:

$$\boldsymbol{y} = h(\boldsymbol{x}) \tag{1}$$

109 where $\boldsymbol{x} = [x_1, x_2, \cdots, x_n]$ denotes a row vector of n input parameters; $\boldsymbol{y} = [y_1, y_2, \cdots, y_m]$ means a row
110 vector of m output features; $h(\cdot)$ means the simulator. The output features herein can be either scalar-
111 valued modal responses or time signals. In the latter case, $\boldsymbol{y}$ is replaced to be $\mathbf{y} = [\boldsymbol{y}_1, \boldsymbol{y}_2, \cdots, \boldsymbol{y}_m]$, with
112 $\boldsymbol{y}_i = [y_i(0), y_i(1), \cdots, y_i(t)]^T, \forall i = 1, 2, \cdots, m$, where t indicates the time parameter. The simulator $h(\cdot)$
113 can be either high-fidelity models, e.g., FE models, or approximated surrogate models.
114   Uncertainties involved in the system are first characterized by representing the input parameters
115 as random variables, and are then propagated through the simulator to the output features. This can
116 be typically achieved by randomly generating the multiple sets of the parameters and corresponding
117 output features. Let the sample size be N_{sim}, the simulator h is evaluated N_{sim} times for obtaining the
118 sample set of the simulated features $\mathbf{Y}_{\text{sim}} \in \mathbb{R}^{N_{\text{sim}} \times m}$:

$$\mathbf{Y}_{\text{sim}} = \left[\mathbf{y}^{(1)}, \mathbf{y}^{(2)}, \cdots, \mathbf{y}^{(N_{\text{sim}})}\right]^T, \text{with } \mathbf{y}^{(k)} = \left[y_1^{(k)}, y_2^{(k)}, \cdots, y_m^{(k)}\right], \forall k = 1, 2, \cdots, N_{\text{sim}} \tag{2}$$

119 in the case that the output features are given as the modal responses. $\mathbf{Y}_{\text{sim}}$ can be simply extended to
120 $\mathbf{Y}_{\text{sim}} \in \mathbb{R}^{N_{\text{sim}} \times m \times (t+1)}$ for the time signals case.
121   In addition to the simulated features, corresponding observed features are also necessary in the
122 model updating. Let the number of observations be N_{obs}, the sample set of the observed features $\mathbf{Y}_{\text{obs}}$
123 possesses a same structure as Eq. (2), but only the number of rows is changed from N_{sim} to N_{obs}. The
124 stochastic model updating is then aimed at minimizing the stochastic discrepancy between $\mathbf{Y}_{\text{sim}}$ and
125 $\mathbf{Y}_{\text{obs}}$ by calibrating the joint probability distribution of the parameters.
126   To quantify the discrepancy between $\mathbf{Y}_{\text{sim}}$ and $\mathbf{Y}_{\text{obs}}$, the Bhattacharyya distance-based UQ metric
127 is employed in this study. The original definition of the Bhattacharyya distance is given as [21]:

$$d_B(\mathbf{Y}_{\text{sim}}, \mathbf{Y}_{\text{obs}}) = -\log\left[\int_{\mathbb{y}} \sqrt{f_{\mathbf{Y}_{\text{sim}}}(\boldsymbol{y}) f_{\mathbf{Y}_{\text{obs}}}(\boldsymbol{y})} \, \mathrm{d}\boldsymbol{y}\right] \tag{3}$$

128 where $f_{(\cdot)}(\boldsymbol{y})$ means the probability density function (PDF) of the output features $\boldsymbol{y}$; $\mathbb{y}$ is the support
129 domain of the output features which comprises m-dimensional space for the modal responses but the
130 $\{m \times (t+1)\}$-dimensional space for the time signals. Eq. (3) indicates the Bhattacharyya distance is a
131 measure of the overlap between the two probability distributions. Hence, it is capable to consider not
132 only mean information but whole statistical information of two different sample sets. However, the
133 direct evaluation of Eq. (3) is usually impractical since precisely estimating the joint PDF of the output
134 features is non-trivial due to the necessity of time-consuming repeated model evaluations or the very
135 limited number of available measurement data. To overcome this issue, Bi et al. [11] proposes the so-
136 called binning algorithm to evaluate the probability mass function (PMF) of the given sample sets, so
137 that the discrete Bhattacharyya distance is utilized instead [22]:

$$d_B(\mathbf{Y}_{\text{sim}}, \mathbf{Y}_{\text{obs}}) = -\log\left\{\sum_{j=1}^{N_{\text{bin}}} \sqrt{P_{\mathbf{Y}_{\text{sim}}}^{(j)} P_{\mathbf{Y}_{\text{obs}}}^{(j)}}\right\} \tag{4}$$

138 where N_{bin} denotes the total number of bins; $P_{(\cdot)}^{(j)}$ denotes the PMF value of the output features at the
139 jth bin. In the binning algorithm, a grid is created in the whole support domain of the output features,
140 and thus the total number of bins would be $N_{\text{bin}} = n_{\text{bin}}^m$ for the modal responses and $N_{\text{bin}} = n_{\text{bin}}^{m \times (t+1)}$
141 for the time signals, where n_{bin} indicates the number of bins for each output feature. One can refer to
142 Ref. [11] for the detailed procedure of the binning algorithm. The discrete Bhattacharyya distance has
143 been demonstrated to be effective in relatively low-dimensional problems (e.g., the dimension is less
144 than six).

145 On the other hand, even the evaluation of Eq. (4) is still impractical for the very high-dimensional
146 problems where the output features comprise time signals, since the number of bins is exponentially
147 increasing with the number of dimensions because of the so-called curse of dimensionality. To tackle
148 this issue, Kitahara et al. [14] proposes a dimension reduction procedure to employ the Bhattacharyya
149 distance for the comparison of two different time signals, consisting of the following steps:

150 1) Define the common window length L for $\mathbf{Y}_{\text{sim}}$ and $\mathbf{Y}_{\text{obs}}$. Divide them into three-dimensional
151 sub-arrays $\mathbf{Y}_{\text{sim}}^s \in \mathbb{R}^{N_{\text{sim}} \times m \times L}$ and $\mathbf{Y}_{\text{obs}}^s \in \mathbb{R}^{N_{\text{obs}} \times m \times L}$, $\forall s = 1, \cdots, \lfloor (t+1)/L \rfloor$, where $\lfloor \cdot \rfloor$ denotes
152 the lower integer of the investigated values;
153 2) Compute the root mean square (RMS) matrices $\mathbf{R}_{\mathbf{Y}_{\text{sim}}}^s \in \mathbb{R}^{N_{\text{sim}} \times m}$ of each sub-array $\mathbf{Y}_{\text{sim}}^s$ along
154 its third dimension and obtain the sample set of the RMS values $\mathbf{R}_{\mathbf{Y}_{\text{sim}}} \in \mathbb{R}^{N_{\text{sim}} \times m \times \lfloor (t+1)/L \rfloor}$. Do
155 similar procedure for the observed features and obtain $\mathbf{R}_{\mathbf{Y}_{\text{obs}}} \in \mathbb{R}^{N_{\text{obs}} \times m \times \lfloor (t+1)/L \rfloor}$;
156 3) Evaluate in total $\lfloor (t+1)/L \rfloor$ Bhattacharyya distances d_B^s between two sample sets $\mathbf{R}_{\mathbf{Y}_{\text{sim}}}^s$ and
157 $\mathbf{R}_{\mathbf{Y}_{\text{obs}}}^s$ using Eq. (4);
158 4) Employ the RMS value of the set of the Bhattacharyya distances, R_{d_B}, as the UQ metric.

159 The authors' experience shows that $L = (0.02 \sim 0.03) \cdot t$ is the reasonable choice for the window length
160 L, and such choice indicates that each window contains $2 \sim 3$ % of the time signals. As such, the time
161 signals are degraded to a series of RMS values, the above defined Bhattacharyya distance-based UQ
162 metric has been demonstrated to be able to quantify the uncertainty characteristics of the entire time
163 signals [14].

164 *2.2. Staircase density functions*

165 Let the input parameter x_i, $\forall i = 1, \cdots, n$, be a random variable having the support domain $[\underline{x}_i, \overline{x}_i]$
166 and a quadruple of the hyper-parameters $\boldsymbol{\theta}_{x_i} = [\mu_i, m_{2i}, \widetilde{m}_{3i}, \widetilde{m}_{4i}]$ consisting of the mean μ_i, variance
167 m_{2i}, skewness $\widetilde{m}_{3i}$, and kurtosis $\widetilde{m}_{4i}$. The skewness $\widetilde{m}_{3i}$ and kurtosis $\widetilde{m}_{4i}$ are defined as ratios of the
168 variance to the third and fourth central moments by $\widetilde{m}_{3i} = m_{3i}/m_{2i}^{3/2}$ and $\widetilde{m}_{4i} = m_{4i}/m_{2i}^2$, respectively.
169 The feasibility condition for the existence of x_i can be defined as moment constraints given by a series
170 of inequalities $\Theta_i = \{\boldsymbol{\theta}_{x_i} : g(\boldsymbol{\theta}_{x_i}) \leq 0\}$, and their components are summarized in Table 1 [23,24].

171 **Table 1.** Moment constraints for the existence of staircase density functions.

Hyper-parameters	Moment constraints
Mean μ_i	$g_1 = \underline{x}_i - \mu_i$
	$g_2 = \mu_i - \overline{x}_i$
Variance m_{2i}	$g_3 = -m_{2i}$
	$g_4 = m_{2i} - v_i$
Skewness $\widetilde{m}_{3i}$	$g_5 = m_{2i}^2 - m_{2i}(\mu_i - \underline{x}_i)^2 - \widetilde{m}_{3i} m_{2i}^{3/2}(\mu_i - \underline{x}_i)$
	$g_6 = \widetilde{m}_{3i} m_{2i}^{3/2}(\overline{x}_i - \mu_i) - m_{2i}(\overline{x}_i - \mu_i)^2 + m_{2i}^2$
	$g_7 = 4m_{2i}^2 + \widetilde{m}_{3i}^2 m_{2i}^3 - m_{2i}^2(\overline{x}_i - \underline{x}_i)^2$
	$g_8 = 6\sqrt{3}\widetilde{m}_{3i} m_{2i}^{3/2} - (\overline{x}_i - \underline{x}_i)^3$
	$g_9 = -6\sqrt{3}\widetilde{m}_{3i} m_{2i}^{3/2} - (\overline{x}_i - \underline{x}_i)^3$
Kurtosis $\widetilde{m}_{4i}$	$g_{10} = -\widetilde{m}_{4i} m_{2i}^2$
	$g_{11} = 12\widetilde{m}_{4i} m_{2i}^2 - (\overline{x}_i - \underline{x}_i)^4$
	$g_{12} = \left(\widetilde{m}_{4i} m_{2i}^2 - v_i m_{2i} - u_i \widetilde{m}_{3i} m_{2i}^{3/2}\right)(v_i - m_{2i}) + \left(\widetilde{m}_{3i} m_{2i}^{3/2} - \mu_i m_{2i}\right)^2$
	$g_{13} = \widetilde{m}_{3i}^2 m_{2i}^3 + m_{2i}^3 - \widetilde{m}_{4i} m_{2i}^3$

$^{\text{a}}$ $u_i = \underline{x}_i + \overline{x}_i - 2\mu_i$ and $v_i = (\mu_i - \underline{x}_i)(\overline{x}_i - \mu_i)$.

172   Let the bounded support domain $[\underline{x}_i, \overline{x}_i]$ equally partitioned into n_b subintervals with the length
173     $\kappa = (\overline{x}_i - \underline{x}_i)/n_b$, x_i can be considered as a staircase random variable, and then its PDF $f_{x_i}(x)$ can be
174   expressed as [17]:

$$f_{x_i}(x) = \begin{cases} l^j & \forall x \in (x_i^j, x_i^{j+1}], \forall j = 1, 2, \cdots, n_b \\ 0 & \text{otherwise} \end{cases} \tag{5}$$

175   where l^j is the PDF value of the jth bin; $x_i^j = \underline{x}_i + (j-1)\kappa$ is the left partitioning point of the jth bin.
176   It is noted that l^j holds that $l^j \geq 0$ for all the bins and $\kappa \sum_{j=1}^{n_b} l^j = 1$. The PDF values $\boldsymbol{l}_i$ are obtained by
177   solving the following optimization problem [17]:

$$\hat{\boldsymbol{l}}_i = \underset{l \geq 0}{\mathrm{argmin}} \left\{ J(\boldsymbol{l}) : \sum_{j=1}^{n_b} \int_{x_i^j}^{x_i^{j+1}} x l^j dx = \mu_i, \sum_{j=1}^{n_b} \int_{x_i^j}^{x_i^{j+1}} (x - \mu_i)^r l^j dx = m_{ri}, r = 2, 3, 4 \right\} \tag{6}$$

178   where $J(\cdot)$ is an arbitrary selected cost function expressed as:

$$J(\boldsymbol{l}) = \boldsymbol{l}^T \mathbf{I} \boldsymbol{l} \tag{7}$$

179   where $\mathbf{I}$ means the identity matrix. This cost function leads to the resultant staircase random variables
180   minimizing the squared sum of the likelihood at each bin. Based on the moment matching constraints,
181   Eq. (6) can be written as [17]:

$$\hat{\boldsymbol{l}}_i = \underset{l \geq 0}{\mathrm{argmin}} \{ J(\boldsymbol{l}) : \mathbf{A}(\boldsymbol{\theta}_{x_i}, n_b) \boldsymbol{l} = \boldsymbol{b}(\boldsymbol{\theta}_{x_i}), \boldsymbol{\theta}_{x_i} \in \Theta_i \} \tag{8}$$

182   where

$$\mathbf{A} = \begin{bmatrix} \kappa \boldsymbol{e} \\ \kappa \boldsymbol{c} \\ \kappa \boldsymbol{c}^2 + \kappa^3/12 \\ \kappa \boldsymbol{c}^3 + \kappa^3 \boldsymbol{c}/4 \\ \kappa \boldsymbol{c}^4 + \kappa^3 \boldsymbol{c}^2/2 + \kappa^5/80 \end{bmatrix}, \text{and } \boldsymbol{b} = \begin{bmatrix} 1 \\ \mu_i \\ \mu_i^2 + m_{2i} \\ \widetilde{m}_{3i} m_{2i}^{3/2} + 3\mu_i m_{2i} + \mu_i^3 \\ m_{4i} m_{2i}^2 + 4\widetilde{m}_{3i} m_{2i}^{3/2} \mu_i + 6 m_{2i} \mu_i^2 + \mu_i^4 \end{bmatrix}$$

183   where $\boldsymbol{c}$ means a column vector of the centre of the bin $c_j = (x_i^j + x_i^{j+1})/2$; $\boldsymbol{c}^n$ denotes the component
184   wise nth power of $\boldsymbol{c}$; $\boldsymbol{e}$ refers to a vector of ones.

185   The convexity of the optimization problem in Eq. (8) enables the fast computation of the staircase
186   density heights. In addition, a relatively small value of n_b (e.g., $n_b = 25 \sim 50$) is enough for obtaining
187   practically smooth distribution shapes for the PMF evaluation, which makes the computation further
188   faster. These features are particularly appropriate for the stochastic updating, where the tremendous
189   number of computations of the probability distributions is necessary. Furthermore, staircase density
190   functions enable to flexibly approximate a broad range of distributions arbitrary close, such as highly
191   skewed and/or multi-modal distributions. Therefore, they can serve as a distribution-free uncertainty
192   characterization model of the parameters whose distribution families cannot be determined.

193   *2.3. Gaussian copula function*

194   Copula functions couple the multivariate joint cumulative distribution function (CDF) with its
195   one-dimensional marginal CDFs. Conversely, copula functions are also seen as the multivariate joint
196   CDFs whose one-dimensional marginal CDFs follow a uniform distribution on the interval of [0, 1].
197   According to Sklar's theorem [25], the bivariate joint CDF of two random variables x_1 and x_2 can be
198   expressed as:

$$F_{\mathbf{x}}(x_1, x_2) = C \left(F_{x_1}(x_1), F_{x_2}(x_2) \right) \tag{9}$$

199   where $F_{x_1}(x_1)$ and $F_{x_2}(x_2)$ are the marginal CDFs of x_1 and x_2, respectively; $C \left(F_{x_1}(x_1), F_{x_2}(x_2) \right)$ is the
200   copula function. From Eq. (9), the bivariate joint PDF of x_1 and x_2 is then written as:

$$f_{\mathbf{x}}(x_1, x_2) = c \left(F_{x_1}(x_1), F_{x_2}(x_2) \right) f_{x_1}(x_1) f_{x_2}(x_2) \tag{10}$$

201   where $c \left(F_{x_1}(x_1), F_{x_2}(x_2) \right)$ denotes the copula density function given as:

$$c\left(F_{x_1}(x_1), F_{x_2}(x_2)\right) = c(u_1, u_2) = \frac{\partial^2 c(u_1, u_2)}{\partial u_1 \partial u_2} \tag{11}$$

202 Theoretically, the joint distribution of x_1 and x_2 can be fully and uniquely represented by Eqs. (9) and
203 (10) if the marginal distributions of x_1 and x_2, and the copula function are given.

204 　　There are many copula function types in the literature, including the Gaussian, t, Frank, Gumbel,
205 and Clayton copula functions. They are characterized by their own dependence structures. The latter
206 three types of copula function can be referred to as Archimedean copulas. The Archimedean copulas
207 have only a single parameter, and thus cannot provide the general dependence structure among more
208 than two random variables. Alternatively, the general dependence structure is often modeled by the
209 pair-copula decomposition introduced as a canonical vine copula [26]. Conversely, the Gaussian and
210 t copulas, which belong to elliptical copulas, can be straightforwardly generalized to the multivariate
211 case. Particularly, the Gaussian copula function is most widely used since it only needs the correlation
212 matrix to determine the dependence structure.

213 　　In this study, the joint probability distribution of the input parameters x is finally characterized
214 by the combination of the Gaussian copula function and staircase density functions as:

$$\begin{aligned} F_\mathbf{x}(x) &= C_G\left(F_{x_1}(x_1), F_{x_2}(x_2), \cdots, F_{x_n}(x_n); \boldsymbol{\rho}\right) \\ &= \Phi_\rho\left(\Phi^{-1}\left(F_{x_1}(x_1)\right), \Phi^{-1}\left(F_{x_2}(x_2)\right), \cdots, \Phi^{-1}\left(F_{x_n}(x_n)\right)\right) \end{aligned} \tag{12}$$

215 where C_G indicates the Gaussian copula function; $\boldsymbol{\rho}$ indicates the correlation matrix; Φ_ρ indicates the
216 multivariate standard normal CDF with $\boldsymbol{\rho}$; Φ^{-1} indicates the inverse function of the standard normal
217 CDF. It is noted that each marginal CDF $F_{x_i}(x_i)$ can be described by the empirical CDF of the staircase
218 density function $f_{x_i}(\cdot)$, for $i = 1, 2, \cdots, n$. The correlation matrix $\boldsymbol{\rho}$ can be expressed as:

$$\boldsymbol{\rho} = \begin{bmatrix} 1 & \rho_{12} & \rho_{13} & \cdots & & \rho_{1n} \\ \rho_{12} & 1 & \rho_{23} & \cdots & & \rho_{2n} \\ \rho_{13} & \rho_{23} & \ddots & \cdots & & \vdots \\ \vdots & \vdots & \vdots & 1 & & \rho_{n-1n} \\ \rho_{1n} & \rho_{2n} & \cdots & \rho_{n-1n} & & 1 \end{bmatrix} \tag{13}$$

219 where ρ_{ij}, for $i = 1, 2, \cdots, n - 1$ and $j = i + 1, \cdots, n$, means the correlation coefficient. The range of each
220 correlation coefficient can reach [-1, 1]. The correlation matrix $\boldsymbol{\rho}$ should be the symmetric and positive
221 semi-definite matrix. Hence, the feasibility condition for the existence of the Gaussian copula function
222 can be defined by the correlation coefficient constraint $\mathcal{P} = \{\boldsymbol{\rho}: \text{chol}(\boldsymbol{\rho}) \neq \emptyset\}$, where $\text{chol}(\cdot)$ means the
223 Cholesky factorization.

224 **3. Distribution-free stochastic model updating**

225 *3.1. Bayesian model updating of the joint probabilistic distribution*

226 　　In the proposed stochastic updating framework, the well-known Bayesian inference is utilized.
227 It is based on the Bayes' theorem [27]:

$$P(\boldsymbol{\vartheta}|\mathbf{Y}_{\text{obs}}) = \frac{P_L(\mathbf{Y}_{\text{obs}}|\boldsymbol{\vartheta})P(\boldsymbol{\vartheta})}{P(\mathbf{Y}_{\text{obs}})} \tag{14}$$

228 where $P(\boldsymbol{\vartheta})$ denotes the prior PDF of the parameters to be inferred $\boldsymbol{\vartheta}$ that is determined by the initial
229 knowledge of the system and expert judgement; $P(\boldsymbol{\vartheta}|\mathbf{Y}_{\text{obs}})$ means the posterior PDF of $\boldsymbol{\vartheta}$ conditional
230 to the measurements, representing the updated knowledge of $\boldsymbol{\vartheta}$; $P(\mathbf{Y}_{\text{obs}})$ indicates the normalization
231 factor (evidence) ensuring the integral of the posterior distribution equal to one; $P_L(\mathbf{Y}_{\text{obs}}|\boldsymbol{\theta})$ indicates
232 the likelihood function of $\mathbf{Y}_{\text{obs}}$ that is defined as the PDF values of the measurements conditional to
233 each instance of $\boldsymbol{\vartheta}$.

234 　　To calibrate the joint probabilistic distribution of the parameters x given by Eq. (13), the hyper-
235 parameters of the staircase density functions $\boldsymbol{\theta}_{x_i}$, for $i = 1, \cdots, n$, and the correlation coefficients of the
236 Gaussian copula function ρ_{ij}, for $i = 1, \cdots, n - 1$ and $j = i + 1, \cdots, n$, are considered to be the inferred
237 parameters $\boldsymbol{\vartheta}$. Based on the moment constraints Θ_i, the support domains of $\boldsymbol{\theta}_{x_i}$ can be determined as:

$$\mu_i \in [\underline{x}_i, \overline{x}_i], m_{2i} \in \left[0, \frac{(\overline{x}_i - \underline{x}_i)^2}{4}\right], m_{3i} \in \left[-\frac{(\overline{x}_i - \underline{x}_i)^3}{6\sqrt{3}}, \frac{(\overline{x}_i - \underline{x}_i)^3}{6\sqrt{3}}\right], m_{4i} \in \left[0, \frac{(\overline{x}_i - \underline{x}_i)^4}{12}\right] \quad (15)$$

It is noted that the support domains are defined not for the skewness and kurtosis but the third and fourth central moments, since the skewness and kurtosis are conditional on the variance. On the other hand, the support domain of ρ_{ij} is simply defined as [-1, 1]. In this study, it is assumed all parameters to be inferred are independent. Based on these support domains with the moment constraints Θ_i and correlation coefficient constraint P, the prior PDF $P(\boldsymbol{\vartheta})$ can be expressed as:

$$P(\boldsymbol{\vartheta}) = \prod_{i=1}^{n} P(\boldsymbol{\theta}_{x_i}) I_{\Theta_i}(\boldsymbol{\theta}_{x_i}) \cdot \prod_{i=1}^{n-1} \prod_{j=i+1}^{n} P(\rho_{ij}) I_{\mathcal{P}}(\rho_{ij}) \quad (16)$$

where $P(\boldsymbol{\theta}_{x_i})$ and $P(\rho_{ij})$ indicate the prior PDFs of the hyper-parameters and correlation coefficients that are chosen as the uniform distributions on their respective support domains; $I_{\Theta_i}(\boldsymbol{\theta}_{x_i})$ denotes the indicator function of $\boldsymbol{\theta}_{x_i}$, which equals to one if Θ_i is satisfied and otherwise equals to zero; $I_{\mathcal{P}}(\rho_{ij})$ is similarly the indicator function of ρ_{ij}. As such, the proposed stochastic updating framework requires only assumptions on the support domains of the input parameters $\boldsymbol{x}$.

This brings totally $4n + n(n-1)/2$ inferred parameters. However, it is widely recognized that the direct evaluation of the posterior PDF over such a high-dimensional parameter space is not trivial [28]. Hence, the well-known advanced sampling technique, termed transitional Markov chain Monte Carlo (TMCMC) [29], is employed in this study. TMCMC is a sequential procedure sampling from a series of transitional PDFs that will gradually converge to the actual posterior PDF, thus it enables to generate samples from the very complex posterior PDF. One can refer to Refs. [29,30] for more details of the TMCMC algorithm.

3.2. Approximate Bayesian computation

The likelihood function plays a key role in the Bayesian model updating. Utilizing the Bayesian inference in the stochastic updating results in the following theoretical likelihood function:

$$P_L(\mathbf{Y}_{\mathrm{obs}}|\boldsymbol{\vartheta}) = \prod_{k=1}^{N_{\mathrm{obs}}} P(\mathbf{Y}_{\mathrm{obs}}^{(k)}|\boldsymbol{\vartheta}) \quad (17)$$

where $P(\mathbf{Y}_{\mathrm{obs}}^{(k)}|\boldsymbol{\vartheta})$ means the PDF value of the kth observations $\mathbf{Y}_{\mathrm{obs}}^{(k)}$ conditional to each instance of the inferred parameters $\boldsymbol{\vartheta}$. The direct evaluation of Eq. (17), however, is often impractical since it requires the significant number of model evaluations so as to precisely estimate the PDFs of the corresponding model outputs.

The ABC method [12,13] has been successfully employed to overcome this obstacle by replacing the above full likelihood function with an approximate but efficient likelihood function that contains information of both the measurements and inferred parameters $\boldsymbol{\vartheta}$. Various forms of the approximate likelihood functions have been investigated in the literature, such as the Gaussian [31], Epanechnikov [32], and inverse squared error [33] functions. Regardless of the function form, it is essential to utilize the comprehensive UQ metric which can serve as an effective connection between the measurements and inferred parameters. In this study, an approximate likelihood function by the Gaussian function is defined by utilizing the Bhattacharyya distance-based UQ metric as:

$$P_L(\mathbf{Y}_{\mathrm{obs}}|\boldsymbol{\vartheta}) \propto exp\left\{-\frac{d_B^2}{\varepsilon^2}\right\} \quad (18)$$

where ε is the pre-defined width factor, which controls the centralization degree of the posterior PDF. A smaller ε provides a more peaked posterior PDF, which is more likely to converge to its true value but needs more computation cost for convergence. Hence, its choice is based on specific applications, while it is recommended to be within the interval of $[10^{-3}, 10^{-1}]$ [31]. By utilizing the Bhattacharyya distance (or the RMS value R_{d_B} for the time signals case), the proposed likelihood enables to quantify the comprehensive uncertainty characteristics of the model outputs and measurements.

276   The schematic in Fig. 1 illustrates overall framework of the proposed distribution-free stochastic
277   updating procedure. As already mentioned, only the support domains of the parameters are required
278   to perform this framework. Sampling from the prior PDF in Eq. (16) can be achieved by the rejection
279   sampling. TMCMC is then utilized to update the inferred parameters to the posterior PDF using the
280   Bhattacharyya distance-based approximate likelihood. By assigning most probable values (MPVs) of
281   the posterior PDF, the joint probabilistic distribution of the input parameters is finally calibrated such
282   that the stochastic model outputs generated from the joint distribution is capable to recreate wholly
283   the uncertainty characteristics of the target measurements. It is important to note that, the calibrated
284   distribution of the parameters is not necessarily applicable to the reliability analysis so as to estimate
285   the probabilities of rare events, since the parameters are finitely bounded due to the definition of the
286   staircase density functions and a domain where the rare event happens might be excluded.
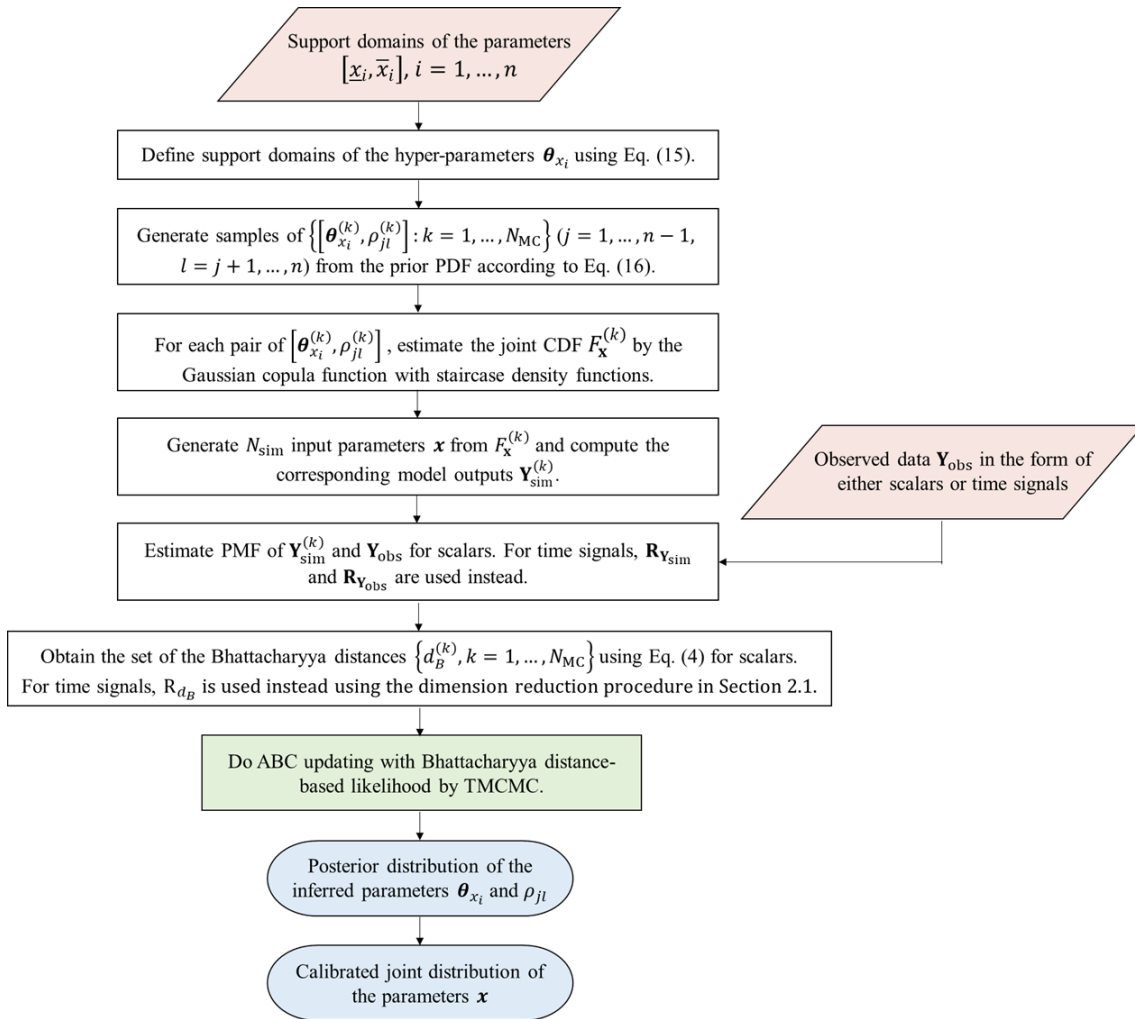
287
288   **Fig. 1.** Schematic of the proposed stochastic model updating framework.

289   **4. Principle and illustrative applications**

290   *4.1. Case study I: The two degree of freedom shear building model*

291   The first case study is performed on a two degree of freedom (DOF) shear building model given
292   in Fig. 2(a). This case study aims at demonstrating the feasibility of the proposed updating procedure
293   for illustrative bivariate case, and how the stochastic model updating fails by ignoring the parameter
294   dependency. This model has been initially introduced by Ref. [28], where the first and second story
295   masses are considered as the fixed values with $m_1 = 16.531 \times 10^3$ kg and $m_2 = 16.131 \times 10^3$ kg. On
296   the other hand, the first and second interstory stiffnesses are characterized as $k_1 = \bar{k}x_1$ and $k_2 = \bar{k}x_2$,
297   where $\boldsymbol{x} = [x_1, x_2]$ indicates the inferred parameters, and $\bar{k} = 29.7 \times 10^6$ N/m is the nominal value.

298   In Ref. [28], the prior PDF $P(x)$ is determined by the pair of uncorrelated lognormal distributions
299   with the MPVs 1.3 and 0.8 for x_1 and x_2, respectively, and the unit standard deviations. By employing
300   the first two natural frequencies $\tilde{f}_1 = 4.31$ Hz and $\tilde{f}_2 = 9.83$ Hz as the observed features, the posterior
301   PDF $P(x|\mathbf{Y}_{\text{obs}})$ is expressed as:

$$P\left(x|[\tilde{f}_1, \tilde{f}_2]\right) \propto exp\left[-\frac{M(x)}{2\sigma^2}\right] P(x) \tag{19}$$

302   where $\sigma = 1/16$ indicates the standard deviation of the prediction error; $M(\cdot)$ is the modal measure-
303   of-fit function expressed as:

$$M(x) = \sum_{j=1}^{2} \lambda^2 \left[\frac{f_j^2(x)}{\tilde{f}_j^2} - 1\right]^2 \tag{20}$$

304   where $\lambda = 1$ is the weight; $f_j(x)$ denotes the jth natural frequency obtained as the model output. Fig.
305   2(b) illustrates the posterior distribution in Eq. (19). It can be seen that the posterior distribution has
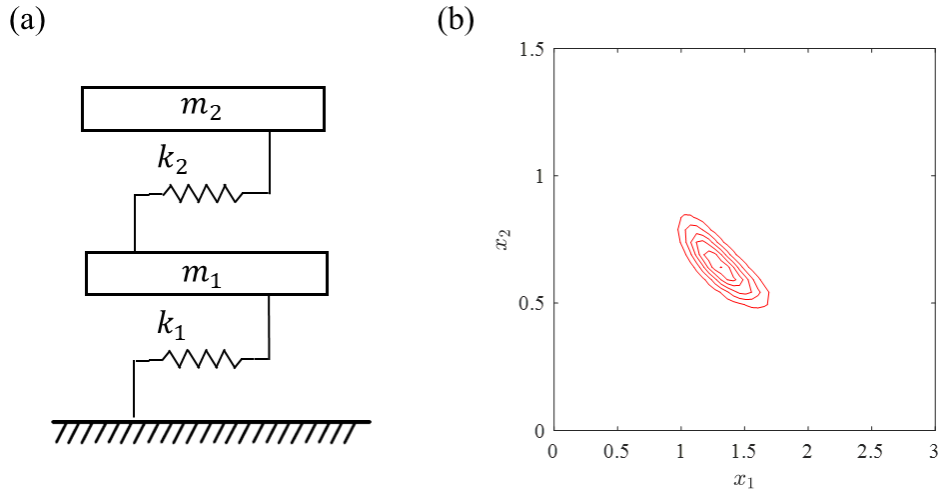306   a clear negative correlation.

(a)   (b)

307
308   **Fig. 2.** (a) 2-DOF shear building model; (b) Posterior distribution in Eq. (19).

309   The aforementioned original problem can be interpreted to aim at estimating the set of plausible
310   values of the input parameters x using the single set of observed features $[\tilde{f}_1, \tilde{f}_2]$ through the Bayesian
311   scheme. Comparatively, the uncertainty characteristics of the input parameters and observed features
312   are altered hereafter to perform the stochastic updating where the joint probability distribution of the
313   input parameters, $F_{\mathbf{x}}(x)$, is calibrated using the multiple sets of the observed features. The target joint
314   distribution is defined to be identical to the posterior distribution in Eq. (19). The number of observed
315   features is set to be $N_{\text{obs}} = 100$; thus, N_{obs} sample sets of the input parameters are generated from the
316   target distribution $P\left(x|[\tilde{f}_1, \tilde{f}_2]\right)$ utilizing TMCMC, and the corresponding observed features $\mathbf{Y}_{\text{obs}}$ are
317   collected by evaluating the model with these sample sets. Note that the target distribution of the input
318   parameters is unknown beforehand in actual. As such, the altered problem is aimed at calibrating the
319   joint distribution of the input parameters to recreate wholly the uncertainty characteristics of $\mathbf{Y}_{\text{obs}}$ by
320   the model outputs generated from the joint distribution.
321   The bounded support domains of x_1 and x_2 are determined as provided in Table 2. The support
322   domain of the hyper-parameters $\boldsymbol{\theta}_{x_1}$ and $\boldsymbol{\theta}_{x_2}$ can be computed using Eq. (15). Let the sample size be
323    $N_{\text{MC}} = 1000$, N_{MC} sets of the initial values of $\boldsymbol{\theta}_{x_1}$ and $\boldsymbol{\theta}_{x_2}$, maintaining the moment constraints Θ_1 and
324   Θ_2, are generated by the rejection sampling while N_{MC} initial values of the correlation coefficient ρ_{12}
325   are arbitrary generated from its support of [-1, 1]. For each set of $[\boldsymbol{\theta}_{x_1}, \boldsymbol{\theta}_{x_2}, \rho_{12}]$, the joint probability
326   distribution of the input parameters x described by the Gaussian copula function with the marginal
327   staircase density functions is determined. The number of bins in staircase density estimation is chosen
328   as $n_b = 25$. At the same time, the number of simulated features is set to be $N_{\text{sim}} = 1000$; hence, N_{sim}
329   sample sets of the input parameters x are generated from each joint distribution $\left\{F_{\mathbf{x}}^{(k)}: k = 1, \cdots, N_{\text{MC}}\right\}$.

330   The corresponding initial simulated features $\mathbf{Y}_{\text{sim}}^{(k)}$ are then collected by evaluating the model for each
331   sample sets of the input parameters. Arbitrary selected initial simulated features are plotted in Fig. 3,
332   together with the target observed features. The figure clearly demonstrates the presence of significant
333   discrepancy between the simulated and observed features, implying the necessity of stochastic model
334   updating for better representation of the uncertainty characteristics of the observed features by means
335   of the model outputs.

336

Table 2. Uncertainty characteristics of the 2-DOF model.

| Parameter	Support domain	Target distribution
x_1	$x_1 \in [0, 3.0]$	The marginal distribution of Eq. (19)
x_2	$x_2 \in [0, 1.5]$	The marginal distribution of Eq. (19)
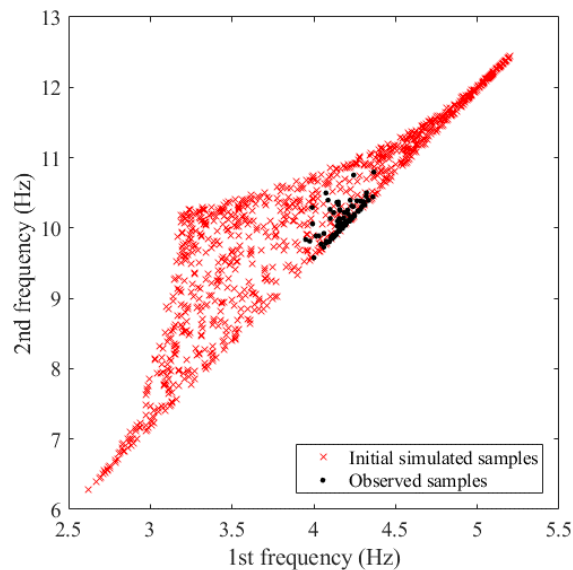
337
338   **Fig. 3.** Observed and initial simulated features.

339   The Bhattacharyya distance is estimated for each set of the simulated features $\mathbf{Y}_{\text{sim}}^{(k)}$. The number
340   of bins in the binning algorithm is chosen to be $n_{\text{bin}} = 5$. Then, the Bayesian model updating of totally
341   nine inferred parameters (i.e., the hyper-parameters $\boldsymbol{\theta}_{x_i} = \{\mu_i, m_{2i}, \tilde{m}_{3i}, \tilde{m}_{4i}\}$, for $i = 1, 2$, as well as the
342   correlation coefficient ρ_{12}) is performed using the Bhattacharyya distance-based likelihood function.
343   The width factor in the likelihood function is set to be $\varepsilon = 0.02$.
344   Fig. 4 shows the posterior PDFs of all the inferred parameters obtained after totally ten TMCMC
345   iterations, together with their target and calibrated values. The target values are estimated based on
346   samples generated from the target joint distribution, while the calibrated values are estimated as the
347   MPVs of the posterior PDFs. These values are summarized in Table 3. It can be seen that the posterior
348   PDFs of all the inferred parameters are significantly updated compared with their uniform priors that
349   are identical to ranges of the horizontal axes of Fig. 4. The posterior supports of the skewnesses and
350   kurtoses are, however, not reduced much from their prior supports, compared with the means and
351   variances, fulfilling the general experience that the higher order moments are difficult to be precisely
352   updated compared with the means [34,35]. Nevertheless, the calibrated values including the kurtoses
353   and the correlation coefficient are in good agreement with their target values with the largest relative
354   error less than 6 %, except for the variance m_{21} and two skewnesses $\tilde{m}_{31}$ and $\tilde{m}_{32}$. The relative errors
355   are shown as percentages in the parentheses after the calibrated values in Table 3. It is noted that, the
356   large relative error in m_{21} can be explained to be caused by its quite small target value, and the error
357   is acceptable to obtain the staircase density function approximating the target distribution as shown
358   in Fig. 5. Meanwhile, the large errors in $\tilde{m}_{31}$ and $\tilde{m}_{32}$ are apparently caused by the wrongly identified
359   signs, whereas their absolute values are close to those of the targets. It should be noted that, the signs
360   of the skewnesses do not strongly affect the uncertainty characteristics of the output features as long
361   as their absolute values are small such that the resultant distributions are almost symmetric. To this
362   end, it is demonstrated that the Bhattacharyya distance can quantify not only mean information but

363 also higher statistical information, i.e., the variances, skewnesses, and kurtoses as well as correlation
364 coefficient.
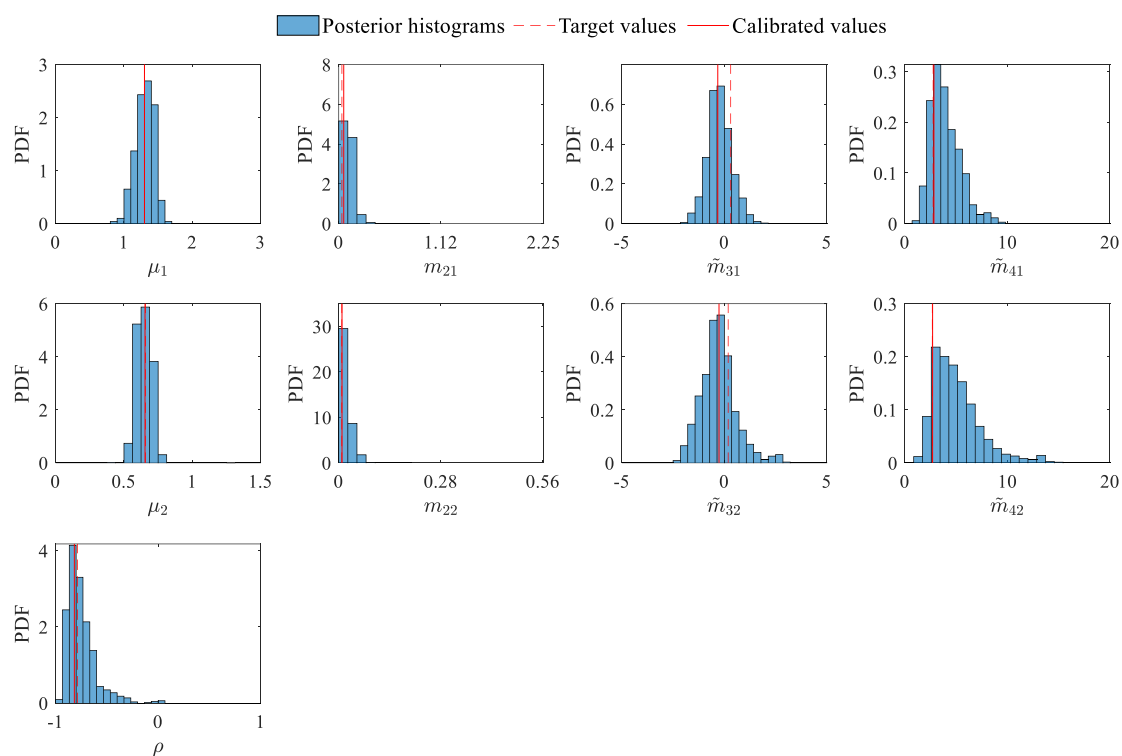
365
366 **Fig. 4.** Posterior PDFs of the inferred parameters.

367 **Table 3.** Calibrated parameters of the 2-DOF model.

Parameter	Target value	Calibrated value	Calibrated value without correlation
μ_1	1.3007	1.3000 (-0.05 %)	1.1214 (-13.78 %)
m_{21}	0.0348	0.0550 (48.85 %)	0.0157 (-54.89 %)
$\widetilde{m}_{31}$	0.3102	-0.3200 (-203.16 %)	0.0022 (-99.29 %)
$\widetilde{m}_{41}$	2.7503	2.8300 (2.90 %)	2.2912 (-16.69 %)
μ_2	0.6568	0.6540 (-0.43 %)	0.7474 (13.79 %)
m_{22}	0.0085	0.0090 (5.88 %)	0.0031 (63.53 %)
$\widetilde{m}_{32}$	0.1866	-0.1780 (-195.39 %)	-0.0849 (-145.50 %)
$\widetilde{m}_{42}$	2.6679	2.7000 (1.20 %)	2.4355 (-8.71 %)
ρ_{12}	-0.7858	-0.8172 (-4.00 %)	–

368 To further demonstrate the results, the sample sets of the input parameters $\boldsymbol{x}$ are generated from
369 the calibrated joint distribution (i.e., the Gaussian copula function with the marginal staircase density
370 functions) and are illustrated in Fig. 5. It can be seen that the samples generated from the calibrated
371 distribution shows good agreement with the target distribution. Meanwhile, the Bayesian updating
372 of only the marginal staircase density functions is also performed to demonstrate how the stochastic
373 model updating fails by ignoring the parameter dependency. The calibrated values of all the hyper-
374 parameters are listed in the last column of Table 3. Most of the parameters denote quite large relative
375 errors compared with those estimated with considering the parameter dependency. The sample sets
376 of the input parameters $\boldsymbol{x}$ generated from the calibrated uncorrelated staircase density functions are
377 also plotted in the figure, which are only distributed in a part of the target distribution, implying the
378 importance of considering the parameter dependency in stochastic model updating.
379 Finally, Fig. 6 illustrates the updated simulated features of f_1 and f_2 that is obtained by assigning
380 the calibrated joint distribution to $\boldsymbol{x}$, together with the initial simulated and target observed features.
381 Moreover, the simulated features are also computed for the case ignoring the parameter dependency,
382 and are provided in the figure. It can be seen that the updated simulated features show a distribution
383 equivalent to the observed features for both cases with and without the parameter dependency, while
384 the former provides better results. It implies that the Bhattacharyya distance metric has a potential to

385 recreate wholly the distribution of the target observed features regardless of the consideration of the
386 parameter dependency. Nonetheless, these results emphasize the importance of consideration of the
387 parameter dependency in the stochastic model updating, because even though the observed features
388 can be ideally quantified, the incompletely calibrated joint distribution of the input parameters could
389 result in an inaccurate prediction of other quantity of interests, which might be important for the risk
390 assessment or design optimization of the target structure.
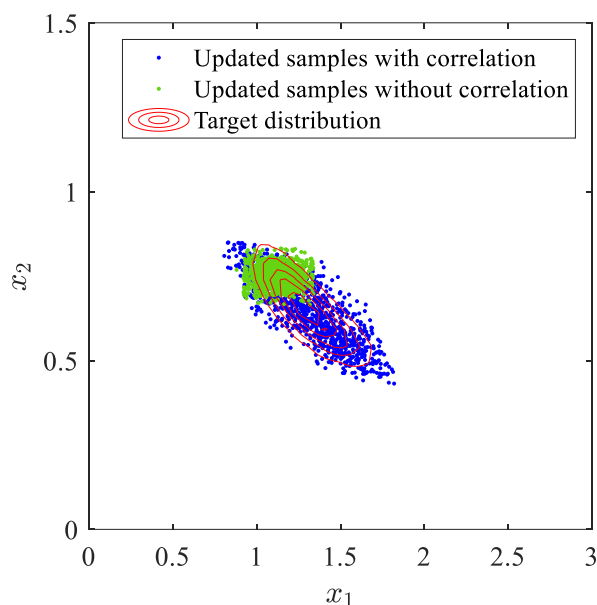

Fig. 5. Updated samples of the input parameters.
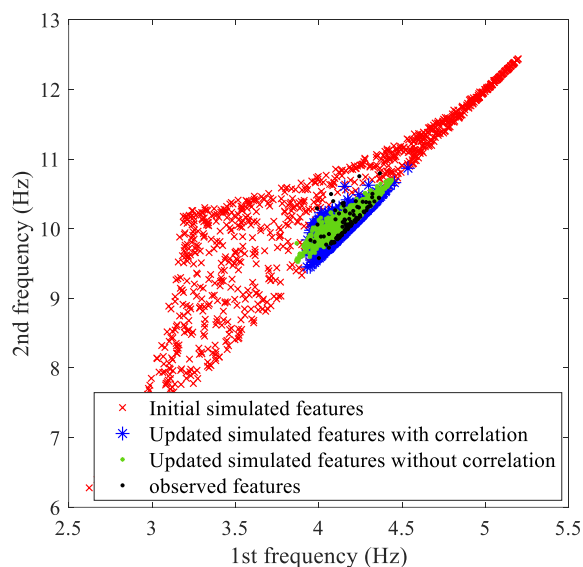
Fig. 6. Updated simulated features.

4.2. Case study II: The three degree of freedom spring-mass system

396   The next case study is performed on a 3-DOF spring-mass system illustrated in Fig. 7. This case
397 study aims at demonstrating the capability of the proposed updating procedure for multivariate case.
398 This numerical system has been employed for demonstrating various stochastic updating techniques
399 [5,11], however, the uncertainty characteristics of the system are changed in this study to demonstrate
400 the proposed approach. The stiffness coefficients k_1, k_2, and k_3 are considered as the uncertain input
401 parameters to be calibrated, whereas the remaining parameters (i.e. k_4 to k_6 and the three masses m_1
402 to m_3) are treated to be the deterministic values: $k_{4-6} = 5.0$ N/m, $m_1 = 0.7$ kg, $m_2 = 0.5$ kg, and $m_3 =$

403 0.3 kg. The first three natural frequencies f_1, f_2, and f_3 are employed as the target output features the
404 uncertainty characteristics of which are driven by the joint probabilistic distribution of k_1, k_2, and k_3
405 that is assumed to be a correlated tri-variate Gaussian distribution. The given support domains of k_1,
406 k_2, and k_3 and the target values of both the hyper-parameters and correlation coefficients are shown
407 in Table 4. It is noted that the support domains are set to cover more than 99.99 % confidence intervals
408 of the target marginal distributions. Such notification is important because the support domain of the
409 target joint distribution is not bounded, differently from the initial case study.
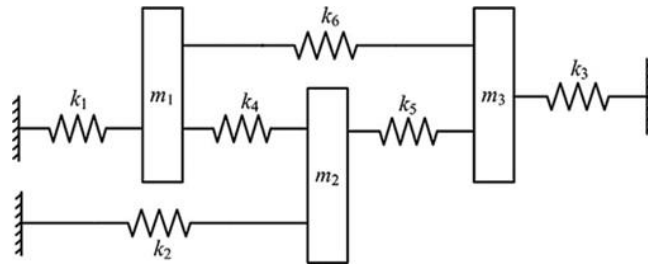
410

411 **Fig. 7.** 3-DOF spring-mass system.

412 **Table 4.** Uncertainty characteristics of the 3-DOF system.

Parameter	Support domain	Target distribution
k_1, k_2, k_3	$k_1 \in [2.5, 5.5]$, $k_2 \in [4.5, 5.5]$, $k_3 \in [5, 7]$	Gaussian, $\mu_1 = 4.0$, $\mu_2 = 5.0$, $\mu_3 = 6.0$, $m_{21} = 0.09$, $m_{22} = 0.01$, $m_{23} = 0.04$, $\rho_{12} = 0$, $\rho_{13} = -0.6$, $\rho_{23} = 0.6$
k_4–k_6, m_1–m_3	Deterministic	–

413 Consider the number of observed features be $N_{\text{obs}} = 500$, N_{obs} sample sets of k_1, k_2, and k_3 are
414 generated from the target joint distribution and then the corresponding observed features $\mathbf{Y}_{\text{obs}}$, which
415 comprise f_1, f_2, and f_3, are collected by evaluating the model with these sample sets.

416 On the other hand, let the sample size be $N_{\text{MC}} = 1000$, N_{MC} sets of the initial values of the hyper-
417 parameters $\boldsymbol{\theta}_{k_1}$, $\boldsymbol{\theta}_{k_2}$, and $\boldsymbol{\theta}_{k_3}$ and the correlation coefficients ρ_{12}, ρ_{13}, and ρ_{23}, satisfying the moment
418 constraints Θ_1, Θ_2, and Θ_3 and the correlation coefficient constraint $\mathcal{P}$, are generated by the rejection
419 sampling in the support domains. For each set of the hyper-parameters and correlation coefficients,
420 the joint distribution of the three stiffness parameters described by the Gaussian copula function with
421 the marginal staircase density functions is determined. The number of bins n_b is set as the same value
422 as that in the first case study. The number of simulated features is set to be $N_{\text{sim}} = 1000$, so that totally
423 N_{sim} sample sets of k_1, k_2, and k_3 are generated from each joint distribution. Then, the corresponding
424 initial simulated features are collected by evaluating the model for each sample sets. Fig. 8 compares
425 the histograms and scatters between the observed features and arbitrary chosen simulated features.
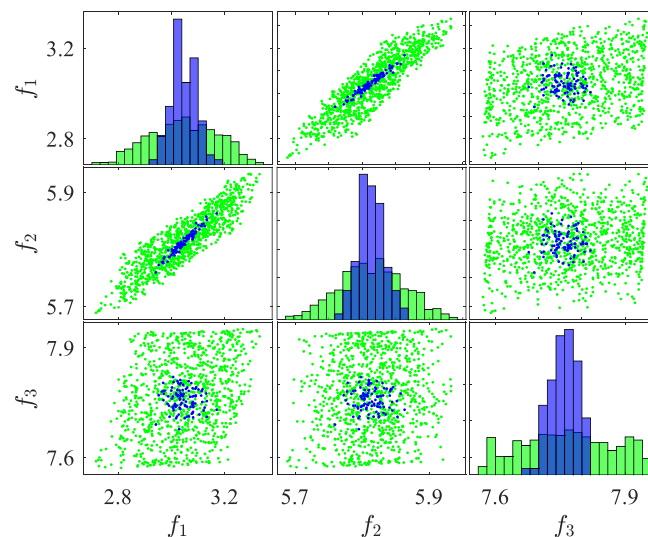
426

427 **Fig. 8.** Observed features in blue and initial simulated features in green, with the unit in Hz.

428   The Bhattacharyya distance is estimated for each set of the initial simulated features. The number
429   of bins n_{bin} is chosen as the same value as that in the first case study. Then, the Bayesian updating of
430   in total 15 inferred parameters, i.e., $\boldsymbol{\theta}_{k_i} = \{\mu_i, m_{2i}, \widetilde{m}_{3i}, \widetilde{m}_{4i}\}$, for $i = 1, 2, 3$, and ρ_{ij}, for $i = 1, 2$ and $j =$
431   $i + 1, 3$, is performed using the Bhattacharyya distance-based likelihood function. The width factor ε
432   is set to be $\varepsilon = 0.01$.

433   By employing in total 17 TMCMC iterations, all the inferred parameters are well updated to the
434   posterior PDFs. The calibrated values (i.e., the MPVs of the posterior PDFs) of all inferred parameters
435   are presented in Table 5, together with the corresponding target values. The relative estimation errors
436   are also provided in the parentheses after the calibrated values. Note that the errors are not provided
437   for the skewnesses and the correlation coefficient ρ_{12} because their true values are zero. It can be seen
438   that the calibrated values of the mean and variance parameters are in good agreement with the target
439   values with the largest relative error less than 5 %. On the contrary, the skewness parameters exhibit
440   differences compared with their target values, especially for $\widetilde{m}_{31}$. However, the calibrated values are
441   small enough for resulting in almost symmetric distributions as similar as the target distributions, as
442   depicted in Fig. 9. The kurtosis parameters also exhibit large errors compared with their target values,
443   whereas these errors are also permissible to obtain reasonable distributions compared with the target
444   distributions as illustrated in Fig. 9. As such, both the skewness and kurtosis parameters are relatively
445   insensitive to the uncertainty characteristics of the target output features, compared with the means
446   and variances. Note that, it does not, however, mean that such higher order moment parameters are
447   always insensitive to the results. As a matter of fact, in the previous example, the kurtosis parameters
448   are precisely updated, implying they are sensitive to the target output features in that example. More
449   importantly, all correlation coefficients are in good agreement with their target values with the largest
450   relative error around 10 %, implying that the proposed procedure is capable to properly capture the
451   correlation structure regardless of no, negative, and positive correlations.

452

Table 5. Calibrated parameters of the 3-DOF system.

| Parameter	Target value	Calibrated value
μ_1	4.0	4.0286 (0.72 %)
m_{21}	0.09	0.0890 (-1.11 %)
$\widetilde{m}_{31}$	0	0.2220
$\widetilde{m}_{41}$	3.0	4.4400 (48.00 %)
μ_2	5.0	5.0035 (0.07 %)
m_{22}	0.01	0.0104 (4.00 %)
$\widetilde{m}_{32}$	0	-0.0500
$\widetilde{m}_{42}$	3.0	3.8100 (27.00 %)
μ_3	6.0	6.0030 (0.05 %)
m_{23}	0.04	0.0410 (2.50 %)
$\widetilde{m}_{33}$	0	-0.0214
$\widetilde{m}_{43}$	3.0	3.9400 (31.33 %)
ρ_{12}	0	-0.0058
ρ_{13}	-0.6	-0.5728 (4.53 %)
ρ_{23}	0.6	0.5398 (10.03 %)

453   The joint distribution of k_1, k_2, and k_3 is then obtained as the Gaussian copula function having
454   the marginal staircase density functions, assigned the calibrated values of the hyper-parameters and
455   correlation coefficients. Fig. 9 shows the marginal CDF of each stiffness, along with the corresponding
456   target marginal distribution. It is noted that, since the marginal distributions are obtained as staircase
457   (i.e., discrete) density functions, the CDFs are estimated from the samples generated according to the
458   staircase density functions, via the kernel density estimation. As can be seen, the estimated staircase
459   density functions are in good agreement with their target marginal distribution, which supports that
460   the aforementioned estimate errors in the skewness and kurtosis parameters are within an allowance
461   for calibrating the joint distribution of the parameters. Nevertheless, it is noted that, in the tail regions,
462   the calibrated distributions, in particular for k_1, remain discrepancy from the target distribution due
463   to the estimate errors in the kurtosis parameters, while the discrepancy in the tail regions do not affect
464   much the model outputs as illustrated in Fig. 10. Moreover, the obtained distributions have bounded

support domains which are identical to ranges of the horizontal axes of Fig. 9 because of the definition
of the staircase density functions, whereas the target Gaussian distributions do not have the bounded
supports. It implies that the proposed procedure does not limit its applicability to the case where the
investigated parameters have bounded supports, however, at the same time, it also indicates that the
calibrated joint distribution cannot be employed for reliability analysis, where the target is estimating
the probabilities of rare events that can be occurred out of the support domains. It is noted that, this
limitation does not prevent the use of the proposed procedure in the stochastic model updating, since
the main motivation of the stochastic model updating is to obtain the model that is capable to describe
the system of interest conditioned on the observed data whereas reliability analysis is only one of the
potential usages of the calibrated model.
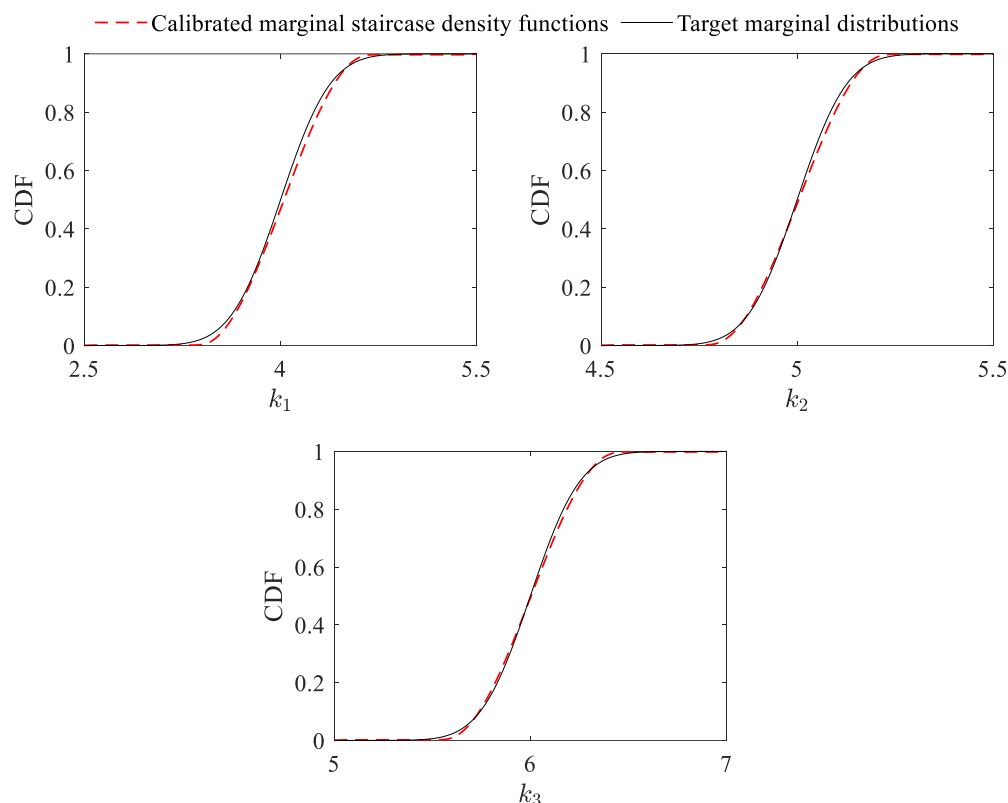
Fig. 9. Calibrated marginal distributions of the input parameters.
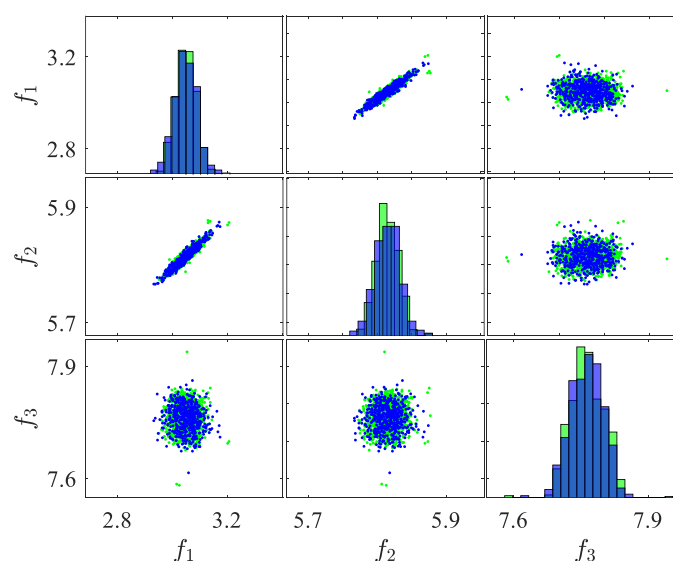
Fig. 10. Observed features in blue and updated simulated features in green, with the unit in Hz.

479   Finally, Fig. 10 compares the histograms and scatters between the target and updated simulated
480   features. Compared with the initial simulated features in Fig. 8, It can be seen that the uncertainties
481   in the three stiffness parameters are correctly calibrated by the proposed procedure and the calibrated
482   model is capable to recreate wholly the uncertainty characteristics of the observed features. As such,
483   the relatively large estimate errors in the higher order moment parameters are permissible, since the
484   objective of the proposed method is not to estimate the individual moment parameters precisely but
485   rather to obtain model outputs that are identical to the observed data, to which some higher moment
486   parameters could be insensitive.

487   **5. Nonlinear dynamic system updating**

488   *5.1. Problem description*

489   The proposed approach is further demonstrated on the updating of nonlinear dynamic systems
490   using the measured time signals. For this purpose, a model updating problem of a reinforced concrete
491   (RC) bridge pier using simulated seismic response data is investigated. The target bridge is a seismic-
492   isolated bridge with lead rubber bearings, designed based on the specifications for highway bridges
493   in Japan [36]. Its structural descriptions are detailed in Table 6. Fig. 11 shows the 2-DOF lumped mass
494   model as the numerical model of the target structure, in which the two lumped masses represent the
495   superstructure and RC pier, and the two horizontal springs denote the rubber bearings and RC pier.
496   The boundary condition at the surface is assumed to be fixed. The nonlinearity of the rubber bearings
497   is characterized by a bilinear model with the ratio of the yield stiffness K_{B1} to the post-yield stiffness
498   K_{B2} of 6.5:1 based on the manual on bearings for highway bridges in Japan [37]. Meanwhile, that of
499   the RC pier is characterized by a bilinear model with the elastoplastic characteristic and the stiffness
500   degradation model, namely Takeda model [38]. The well-known Rayleigh damping model is utilized
501   as the damping model in which the damping ratios of the rubber bearings and RC pier are set to be
502   0 % and 2 %, respectively.

503   **Table 6.** Descriptions of the target bridge pier.

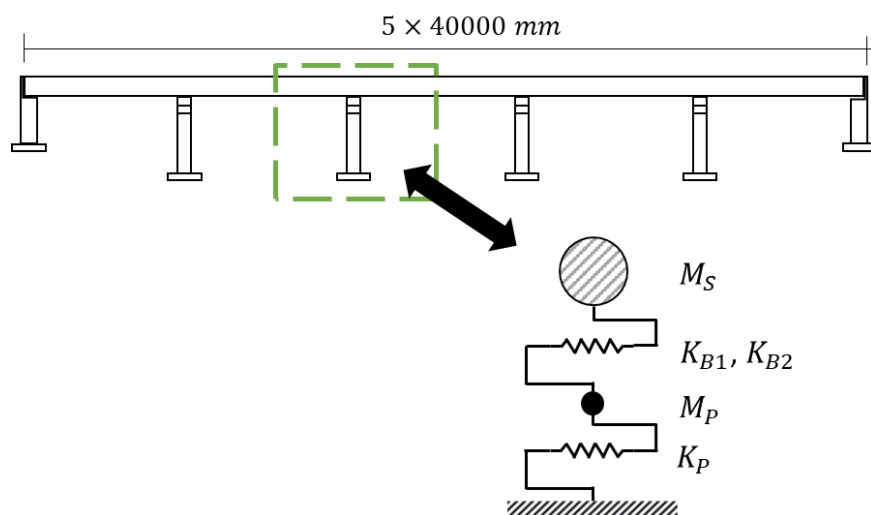|	Structural parameter	Nominal value
Superstructure	Mass M_S (ton)	604.0
Rubber bearings	Yield strength (kN)	1118
	Yield stiffness K_{B1} (kN/m)	40000
	Post-yield stiffness K_{B2} (kN/m)	6000
RC pier	Mass M_P (ton)	346.2
	Yield strength (kN)	3374
	Yield stiffness K_P (kN/m)	110100
	Yield displacement (m)	0.0306

504
505   **Fig. 11.** Numerical modeling of the target bridge pier.

506   The aim of this updating problem is to quantify the uncertainty characteristics of the post-yield
507 stiffness of the rubber bearings, K_{B2}, which governs the nonlinear behaviour of the target bridge pier
508 under strong earthquakes, as well as the remaining stiffnesses K_{B1} and K_P. These three stiffnesses are
509 parameterized as $K_{B1} = \bar{K}_{B1} x_1$, $K_{B2} = \bar{K}_{B2} x_2$, and $K_P = \bar{K}_P x_3$, where $\boldsymbol{x} = [x_1, x_2, x_3]$ are uncertain input
510 parameters, and $\bar{K}_{B1}$, $\bar{K}_{B2}$, and $\bar{K}_P$ are the nominal values shown in Table 6. The other parameters are
511 assumed to be fixed constants with the nominal values. The time-history of the acceleration response
512 at the superstructure subjected to the level-2 type-II-II-1 earthquake introduced in Ref. [36] is used as
513 the target output features. The duration time of the input ground motion is 40 s. Time history analysis
514 of the 2- DOF model is performed using the Newmark β method ($\beta = 1/4$ and $\gamma = 1/2$) with the time
515 step $\Delta t = 0.001$ s. Fig. 12 illustrates the time-history of the acceleration response at the superstructure
516 and the force-displacement responses of the rubber bearings and pier for the case when all parameters
517 are fixed to the nominal values shown in Table 6.
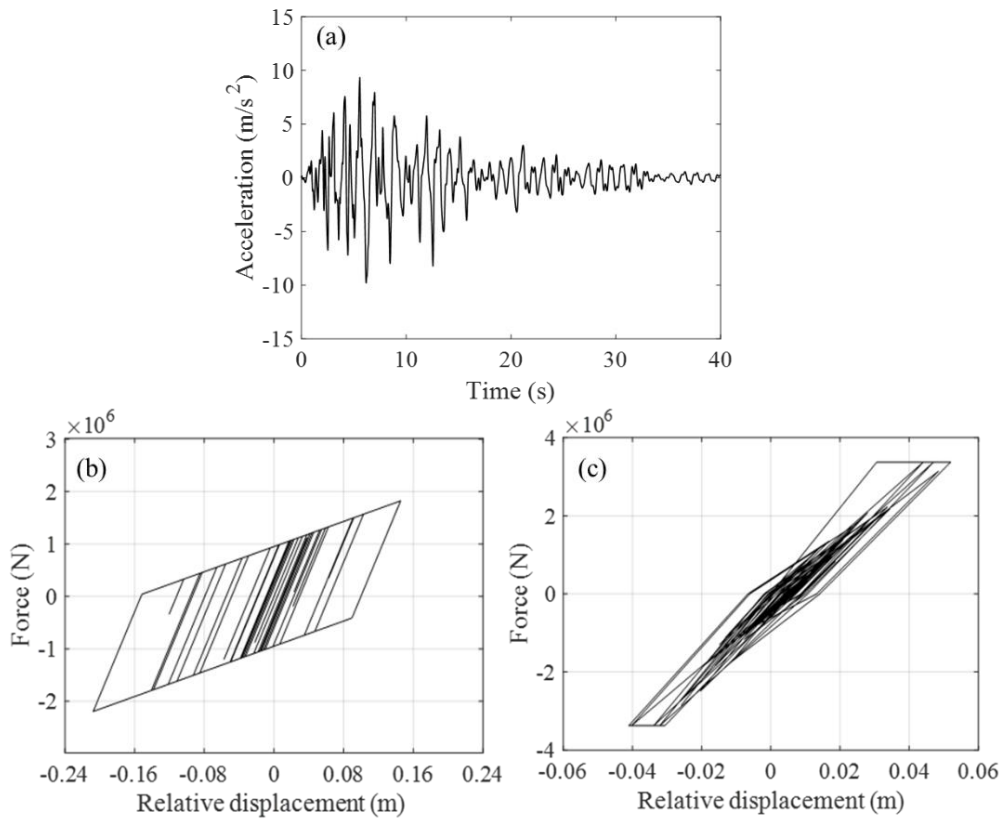
518
519   **Fig. 12.** (a) Time-history of the acceleration response at superstructure; (b) Force-displacement response of
520   rubber bearings; (c) Force-displacement response of RC pier.

521   The target joint distribution of the input parameters $\boldsymbol{x}$ is considered to be a correlated tri-variate
522 Gaussian distribution, in which a positive correlation between x_1 and x_2 (i.e., between the initial and
523 post stiffnesses of the rubber bearings) is introduced. The pre-defined support domains of x_1, x_2, and
524 x_3 and the target values of the hyper-parameters and correlation coefficients are detailed in Table 7.
525 Similar to the previous case study, the support domains are determined to cover more than 99.99 %
526 confidence intervals of their target marginal distributions. Suppose the number of observed features
527 be $N_{\text{obs}} = 100$, N_{obs} sample sets of the input parameters $\boldsymbol{x}$ are generated according to the target joint
528 distribution and then the corresponding observed features $\mathbf{Y}_{\text{obs}}$ of the time-history of the acceleration
529 response at the superstructure, are collected by evaluating the model with these sample sets.

530   **Table 7.** Uncertainty characteristics of the target bridge pier.

Parameter	Support set	Target distribution
x_1, x_2, x_3	$x_1 \in [0.7, 1.3]$, $x_2 \in [0.7, 1.3]$, $x_3 \in [0.7, 1.3]$	Gaussian, $\mu_1 = 1.0$, $\mu_2 = 1.0$, $\mu_3 = 1.0$, $m_{21} = 0.0049$, $m_{22} = 0.0049$, $m_{23} = 0.0049$, $\rho_{12} = 0.8$, $\rho_{13} = 0$, $\rho_{23} = 0$
M_S, M_P	Deterministic	–

531   In this example, totally 13 inferred parameters, i.e., the hyper-parameters $\boldsymbol{\theta}_{x_i} = \{\mu_i, m_{2i}, m_{3i}, m_{4i}\}$,
532 for $i = 1, 2, 3$, and correlation coefficient ρ_{12} is taken into account. Note that the remaining correlation
533 coefficients are assumed to be zero in advance and ignored in the updating procedure. Suppose the
534 sample size be $N_{\text{MC}} = 100$, N_{MC} sets of the hyper-parameters maintaining the moment constraints Θ_1
535 Θ_2, and Θ_3, are generated by the rejection sampling whereas N_{MC} sets of the correlation coefficient are
536 arbitrary generated from the support of [-1, 1]. For each set of $[\boldsymbol{\theta}_{x_1}, \boldsymbol{\theta}_{x_2}, \boldsymbol{\theta}_{x_3}, \rho_{12}]$, the joint probability
537 distribution of the input parameters $\boldsymbol{x}$ is defined as the Gaussian copula function having the marginal
538 staircase density functions. The number of bins n_b is chosen to be $n_b = 50$. The number of simulated
539 features, on the other hand, is set as $N_{\text{sim}} = 500$; hence, N_{sim} sample sets of $\boldsymbol{x}$ are generated from each
540 joint distribution $\left\{F_{\mathbf{x}}^{(k)}: k = 1, \cdots, N_{\text{MC}}\right\}$, and then the corresponding initial simulated features $\mathbf{Y}_{\text{sim}}^{(k)}$ are
541 obtained by evaluating the model with these samples. The window length in the dimension reduction
542 procedure introduced in Section 2.1 is set to be L $= 0.025(t + 1)$, with $t = 40/0.001 = 40000$. Hence,
543 the RMS matrices of both the simulated and observed features, $\mathbf{R}_{\mathbf{Y}_{\text{sim}}^{(k)}}^s$ and $\mathbf{R}_{\mathbf{Y}_{\text{sim}}}^s$, for $\forall s = 1, \cdots, 40$, are
544 defined. Fig. 13 compares the histograms and scatters between the observed and simulated features
545 by employing five arbitrary selected RMS matrices of $s = 30, 7, 6, 9, 37$. The figure demonstrates that
546 the target features show strong nonlinearity, making the updating problem significantly challenging.
547 The Bhattacharyya distance is estimated for each pair of the simulated and observed RMS matrices,
548 and the RMS value of the Bhattacharyya distances, R_{d_B}, is used as the UQ metric in the approximate
549 likelihood. The number of bins n_{bin} is chosen as $n_{\text{bin}} = 10$ while the width factor ε is set as $\varepsilon = 0.01$.
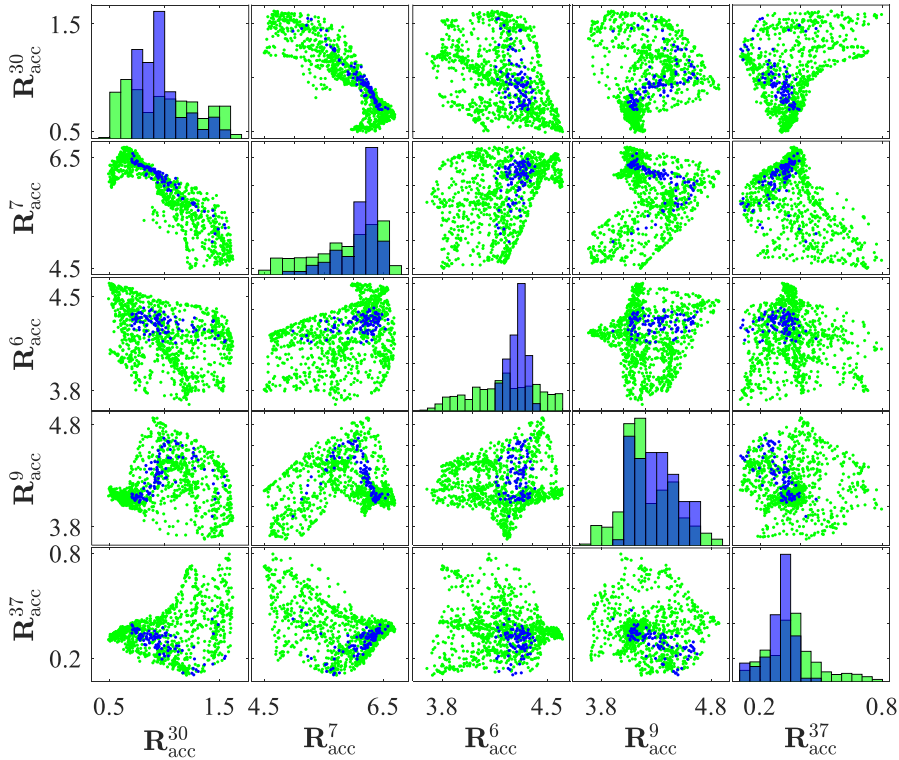
550
551   **Fig. 13.** Observed features in blue and initial simulated features in green, with the unit in m/s^2.

552 *5.2. Results assessment*

553   By employing totally 13 TMCMC iterations, all the inferred parameters are well updated to the
554 posterior PDFs. The calibrated values of the inferred parameters are detailed in Table 8, together with
555 the corresponding target values. The relative estimation errors are also shown in the parentheses after
556 the calibrated values. The calibrated values of all mean parameters and the variance parameter m_{21}
557 are in good agreement with the target values, while the remaining variance parameters exhibit large
558 estimate errors due to their quite small target values. In spite of the large relative errors, the calibrated
559 values of the variance parameters are close to the target values compared with the prior supports and

560   the errors are within an allowance to achieve the model outputs close to the observations. In addition,
561   the skewnesses and kurtoses exhibit differences compared with their target values, while these errors
562   are also within an allowance to achieve the model outputs close to the target observations, as similar
563   as the previous example. Moreover, the positive correlation induced is also captured by the proposed
564   procedure though a certain error is still remained compared with the target value. By assigning these
565   calibrated values, the joint distribution of x is tuned identical to the target distribution.

566   **Table 8.** Calibrated parameters of the target bridge pier model.

Parameter	Target value	Calibrated value
μ_1	1.0	0.9958 (-0.42 %)
m_{21}	0.0049	0.0045 (-4.44 %)
$\widetilde{m}_{31}$	0	-0.1688
$\widetilde{m}_{41}$	3.0	4.3450 (44.83 %)
μ_2	1.0	0.9992 (-0.08 %)
m_{22}	0.0049	0.0065 (32.65 %)
$\widetilde{m}_{32}$	0	0.4050
$\widetilde{m}_{42}$	3.0	3.9500 (31.67 %)
μ_3	1.0	0.9996 (-0.04 %)
m_{23}	0.0049	0.0068 (38.78 %)
$\widetilde{m}_{33}$	0	-0.3025
$\widetilde{m}_{43}$	3.0	4.3960 (46.53 %)
ρ_{12}	0.8	0.6736 (-15.80 %)

567   Finally, Fig. 14 compares the histograms and scatters between the target and simulated features
568   for the five arbitrary selected RMS matrices of $s = 30, 7, 6, 9, 37$. Compared with the initial simulated
569   features in Fig. 13, It can be seen the updated simulated features are identical to the observed features
570   capturing the complicated nonlinear structure. This indicates the feasibility of the proposed approach
571   in the stochastic model updating of nonlinear dynamic systems for recreating wholly the uncertainty
572   characteristics of the target measured time signals, even though the prior knowledge about the joint
573   probability distribution of the model parameters is extremely limited.
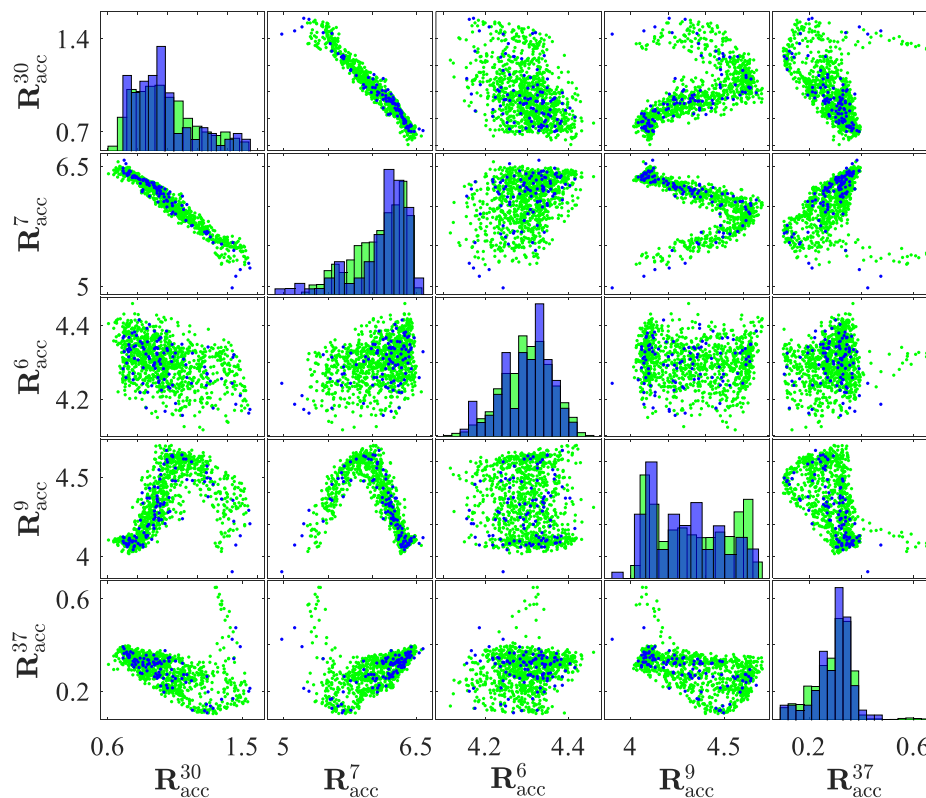
574
575   **Fig. 14.** Observed features in blue and updated simulated features in green, with the unit in m/s^2.

6. Conclusions

This paper presents three contributions for calibrating the joint probabilistic distribution of the correlated parameters through the stochastic model updating by a limited number of measurement data. First, each marginal distribution is characterized by staircase density functions and their hyper-parameters are subjected to be updated. The staircase density functions can flexibly describe a broad range of distributions; thus, no limiting hypotheses on the distribution families is required differently from the most of the stochastic model updating methods. Next, the dependence structure among the parameters are described by the Gaussian copula. The correlation coefficients are also subjected to be updated; thus, even the prior knowledge on the presence of parameter dependencies is not required. Finally, the Bhattacharyya distance-based UQ metric is proposed to define an approximate likelihood capable of quantifying the stochastic discrepancy between the model outputs and measurements. As such, the inferred parameters, i.e., the hyper-parameters and correlation coefficients are successfully updated through the Bayesian model updating. Two exemplary applications and followed nonlinear dynamic system updating problem demonstrate the feasibility of the proposed updating framework and the importance of considering the parameter dependency in the stochastic model updating.

However, open problems still exist. First, the cost function in the optimization problem solved for estimating the staircase density function is solely selected in this study. The staircase density that attains other optimality criteria, such as the maximal entropy, can be similarly formulated, but further studies are necessary to investigate the most suitable choice of the cost function for model updating. Second, the Gaussian copula might not be suitable if the parameters demonstrate a strong nonlinear dependency. The assumption on the copula function type introduces another source of uncertainty, i.e., the model bias, and such uncertainty should be quantified by, for instance, the Bayesian model class selection. These two challenges will be addressed in the future work.

References

1. J.E. Mottershead, M, Ling, M.I. Friswell, The sensitivity method in finite element model updating: A tutorial, Mech. Syst. Signal Process. 25 (2011) 2275-2296.

2. E. Patelli, Y, Govers, M. Broggi, H.M. Gomes, M. Ling, J.E. Mottershead, Sensitivity or Bayesian model updating: a comparison of techniques using the DLR AIRMOD test data. Arch. Appl. Mech. 87 (2017) 905-925.

3. J.E. Mottershead, M.I. Friswell, Model Updating In Structural Dynamics. J. Sound Vib. 167 (1993) 347-375.

5. D. Shan, Q. Li, I. Khan, X. Zhou, A novel finite element model updating method based on substructure and response surface model, Eng. Struct. 103 (2015) 147-156.

6. C. Mares, J.E. Mottershead, M.I. Friswell, Stochastic model updating: Part 1—theory and simulated example, Mech. Syst. Signal Process. 20 (2006) 1674-1695.

7. K.K. Sairajan, G.S. Aglietti, Robustness of system equivalent reduction expansion process on spacecraft structure model validation, AIAA J. 50 (2012) 2376-2388.

8. S. Bi, S. Prabhu, S. Cogan, S. Atamturktur, Uncertainty quantification metrics with varying statistical information in model calibration and validation, AIAA J. 55 (2017) 3570-3583.

9. B. Goller, M. Broggi, A. Calvi, G.I. Schuëller, A stochastic model updating technique for complex aerospace structures, Finite Elem. Anal. Des. 47 (2011) 739-752.

| 620 | 10. | Y. Govers, M. Link, Stochastic model updating—Covariance matrix adjustment from |
| 621 | | uncertain experimental modal data, Mech. Syst. Signal Process. 24 (2010) 696-706. |

621   uncertain experimental modal data, Mech. Syst. Signal Process. 24 (2010) 696-706.

622 11. S. Bi, M. Broggi, M. Beer, The role of the Bhattacharyya distance in stochastic model updating,
623   Mech. Syst. Signal Process. 117 (2019) 437-452.

624 12. M.A. Beaumont, W. Zhang, D.J. Balding, Approximate Bayesian computation in population
625   genetics, Genetics 162 (2002) 2025-2035.

626 13. B.M. Turner, T. Van Zandt, A tutorial on approximate Bayesian computation, J. Math. Psychol.
627   56 (2012) 69-85.

628 14. M. Kitahara, S. Bi, M. Broggi, M. Beer, Bayesian model updating in time domain with
629   metamodel-based reliability method, J. Risk Uncertainty Eng. Syst. Part A: Civ. Eng. 7 (2021)
630   04021030.

631 15. L.G. Crespo, S.P. Kenny, The NASA Langley multidisciplinary uncertainty quantification
632   challenge, Mech. Syst. Signal Process. 152 (2021) 107405.

633 16. M. Kitahara, S. Bi, M. Broggi, M. Beer, Nonparametric Bayesian stochastic model updating
634   with hybrid uncertainties, Mech. Syst. Signal Process. 163 (2022) 108195.

635 17. L.G. Crespo, S.P. Kenny, D.P. Giesy, B.K. Stanford, Random variables with moment-matching
636   staircase density function, Appl. Math. Model 64 (2018) 196-213.

637 18. X.S Tang, D.Q. Li, C.B. Zhou, K.K. Phoon, L.M. Zhang, Impact of copulas for modeling
638   bivariate distributions on system reliability, Struct. Safety 44 (2013) 80-90.

639 19. D.Q. Li, L. Zhang, X.S. Tang, W. Zhou, J.H. Li, C.B. Zhou, K.K. Phoon, Bivariate distribution
640   of shear strength parameters using copulas and its impact on geotechnical system reliability,
641   Compt. Geotech. 68 (2015) 184-195.

642 20. X.S Tang, D.Q. Li, C.B. Zhou, K.K. Phoon, Copula-based approaches for evaluatig slope
643   reliability under incomplete probability information, Struct. Safety 52 (2015) 90-99.

644 21. A. Bhattacharyya, On a measure of divergence between two multinominal populations, Indian
645   J. Stat. 7 (1964) 401-406.

646 22. B.K. Patra, R. Launonen, V. Ollikainen, S. Nandi, A new similarity measure using
647   Bhattacharyya coefficient for collaborative filtering in sparse data, Knowledge-Based Syst. 82
648   (2015) 163-177.

649 23. R. Sharma, S. Devi, G. Kapoor, N.S. Barnett, A brief note on some bounds connecting lower
650   order moments for random variables defined on a finite interval, Int. J. Theor. Appl. Sci. 1
651   (2009) 83-85.

652 24. P. Kumar, Moment inequalities of a random variable defined over a finite interval, J. Inequ.
653   Pure. Appl. Math. 3 (2002) 1-11.

654 25. R.B. Nelsen, An Introduction to Copulas; 2nd ed, Springer, New York, 2006.

655 26. L.H. Haff, Parameter estimation for pair-copula constructions, Bernoulli 19 (2013) 462-491.

656 27. J.L. Beck, L.S. Ktafygiotis, Updating models and their uncertainties. I: Bayesian statistical
657   framework, J. Eng. Mech. 124 (1998) 455-461.

658 28. J.L. Beck, S.K. Au, Bayesian updating of structural models and reliability using Markov chain
659   Monte Carlo simulation, J. Eng. Mech. 128 (2002) 380-391.

660 29. J. Ching, Y.C. Chen, Transitional Markov chain Monte Carlo method for Bayesian updating,
661   model class selection, and model averaging, J. Eng. Mech. 133 (2007) 816-832.

662 30. W. Betz, I. Papaioannou, D. Straub, Transitional Markov chain Monte Carlo: Observations and
663   improvements, J. Eng. Mech. 142 (2016).

664 31. E. Patelli, D.A. Alvarez, M. Broggi, M. de Angelis, Uncertanty management in
665   multidisciplinary design of critical safety systems, J. Aerosp. Inf. Syst. 12 (2015) 140-169.

666 32. C. Safta, K. Sargsyan, H.N. Najm, K. Chowdhary, B. Debusschere, L.P. Swiler, M.S. Eldred,
667   Probabilistic methods for sensitivity analysis and calibration in the NASA challenge problem,
668   J. Aerosp. Inf. Syst. 12 (2015) 219-234.

669 33. R. Rocchetta, M. Broggi, Q. Huchet, E. Patelli, On-line Bayesian model updating for structural
670   health monitoring, Mech. Syst. Signal Process. 103 (2018) 174-195.

671 34. P. Li, Z. Lu, Y. Zhao, Bayesian updating of time-dependent structural reliability using the
672   method of moment, J. Risk Uncertainty Eng. Syst. Part A: Civ. Eng. 7 (2021) 04021066.

673 35. B. Liao, R. Zhao, K. Yu, C. Liu, A novel interval model updating framework based on
674   correlation propagation and matrix-similarity method, Mech. Syst. Signal Process. 162 (2022)
675   108039.

676 36. Japan Road Association, Design specifications of highway bridges V: Seismic design,
677   Maruzen, Tokyo, 2016.

678 37. Japan Road Association, Manual on bearings for highway bridges, Maruzen, Tokyo, 2004. (In
679   Japanese).

680 38. T. Takeda, M.A. Sozen, N.N. Nielsen, Reinforced concrete response to simulated earthquakes,
681   J. Struct. Div. 96 (1970) 2257-2573.